IEEE International Workshop on
Virtual and Intelligent Measurement Systems
Budapest, Hungary, May 19-20, 2001.

Three-Dimensional Motion System ("Data-Gloves"): Application for Parkinson's Disease and Essential Tremor

Y Su[1], D Geng[1], C R Allen[1], D Burn[2], G D Bell[3], R Rowland[4]

[1]Department of Electrical and Electronic Engineering, University of Newcastle upon Tyne
[2] Regional Neurosciences Centre, Newcastle General Hospital, Westgate Road

Newcastle upon Tyne, NE1 7RU, UNITED KINDOM

[3]Medical Sciences Faculty, Sunderland University, Kayll Rd Sunderland SR4 7TP

[4]School of Information System, University of East Anglia, Norwich, UNITED KINDOM

Phone: +44 191 2227332, Fax: +44 191

Email: c.r.allen@ncl.ac.uk, URL: http://www.staff.ncl.ac.uk/c.r.allen/

Abstract: ***The accurate modelling and analysis of medical treatment plays an important role in modern medical science. This paper describes an attempt to apply current sensor and control techniques to quantitatively measure significant motion of the human body. By modelling the movement of human hand this system can accurately measure the hand posture and all the phalanges, store the measurements as X,Y, Z absolute positions and the computer can (off-line) compute the movement of the hand and phalanges. By applying dedicated embedded electronics a portable and networked system can be realized which may be used in the clinical assessment of stroke patients or medical conditions such as Parkinson's disease. It can be used as both a training instrument and a tool for medical diagnosis and research, leading to objective analysis of medical conditions involving accurate posture measurement of the human body.***

Keywords**:** ***3D imaging systems, posture data glove sensing, Parkinson's disease [PD], essential tremor [ET], bradykinesia.***

I INTRODUCTION

Attempts to quantify signs of Parkinsonism date back to the 1920's. Methods may be subdivided into objective quantification techniques and subjective assessments. The latter are commonly used in clinical practice and include patient functional disability scales, patient-completed diaries and subjective physician ratings of severity of signs of disease. Accurate assessment of tremor and bradykinesia using objective techniques may, however, improve diagnostic specificity and provide un-biased quantification of therapeutic interventions.

Many objective techniques sample only limited aspects of motor dysfunction. The relationship between pathophysiology, impairment and disability is complex and a problem in one area does not necessarily predict difficulty in another. Existing physiological techniques to record tremor include accelerometry, electromyography (short- or long-term), computer tracking tasks, graphic digitizing tablets and infrared sensor systems (1). Each of these techniques has their drawbacks, and many are very time-consuming to perform. Objective tests for bradykinesia are even less satisfactory, and include the Purdue pegboard, and tapping tests between two counters a fixed distance apart.
In the paper, we intend to introduce novel three-dimensional Motion system, developed from the JSB Medical Imaging System and applying electromagnetic position sensors (hand movement recognition), for use in the recording of upper limb tremors and bradykinesia.

The JSB medical imaging system has achieved success in visualising online the position of endoscopes in the human colon [2]. However, in Parkinson's disease, hand movements are of higher speed (as fast as 4Hz) and more sensor channels are required to provide detailed recording. The original JSB Medical imaging system can not fulfil this speed requirement. Thus, a faster algorithm is required to provide quantitative hand movement measurement. This paper outlines the development of an improved 3D imaging system which achieves this specification and provides additional advantageous features such as a portable unit with networking capabilities based on the Ethernet.

The advanced imaging System will be used together with a "Data-glove" to be worn on the dominant hand of the patient. The objective will then be to characterise patients exhibiting clinically probable PD (according to the UK Parkinson's Disease Brain Bank Criteria [3]) and patients with definite essential tremor (according to the TRIG criteria [4]) during the studies.

The responsiveness of the system to therapeutic intervention will be assessed by recordings of PD and ET patients' hand motion made using the Data-glove.

Virtual reality sensors provide a powerful technology for human-computer interaction (HCI) and have been applied to many fields (5) Their particularly useful feature is that the user may use the technology easily and routinely by using ready-to-wear articles of clothing e.g. headsets or data-gloves. Secondly the VR sensors could be simply plug into a computer system and allow the user uninhibited control and interaction with both the local computer system and, through digital communication channels, users worldwide [6].

Section 2 describes the principle of electromagnetic 3D measurement. Section 3 introduces the mathematical model required to construct the hand model from the measurements. Section 4 shows the results obtained in using the data-gloves and JSB Imaging System and the accuracy. Section 5 analyses the data rate required to sustain a real-time hand moving applet at the remote site. Section 6 discusses the value of this approach for provision of visual simulation for the comparison of the patient before and after the medical treatment. Section 7 is the scenario of the system development

II PRINCPLE OF 3D ELECTRO-MAGNETIC MEASUREMENT

In order to measure the 3D position and orientation of a sensor an alternating current (AC) magnetic field must be applied. Each sensor coil then provides an induced voltage that is proportional to the magnetic field strength. To compute the full 3D position and orientation specification of the sensor coil requires several simultaneous measurements to be made. This has required nine generator magnetic sources to be used, which are arranged in three orthogonal sets placed on a horizontal plane. The imaging system is shown in Figure 1. This system is based on low strength magnetic field capable of capturing the absolute position of the magnetic sensor mounted on the data glove, avoiding the difficulties of calibration of conventional bending sensors. Magnetic field can be generated and detected using low cost device and is considered safe. Also, unlike acoustic and microwave field, the generators do not need to be in contact with the body or require matching media making the system convenient to use (7).

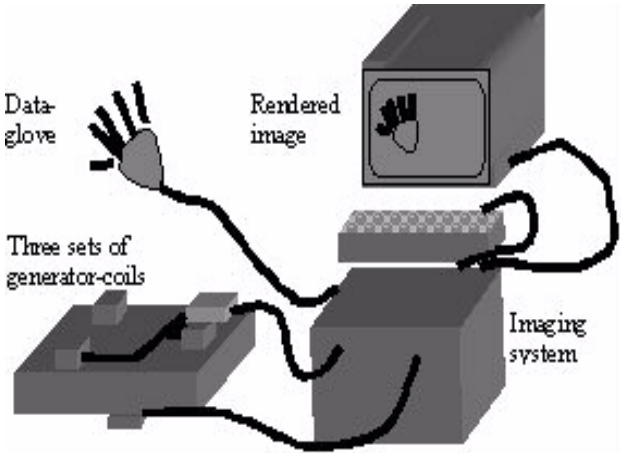

Fig. 1. Imaging System Schematic

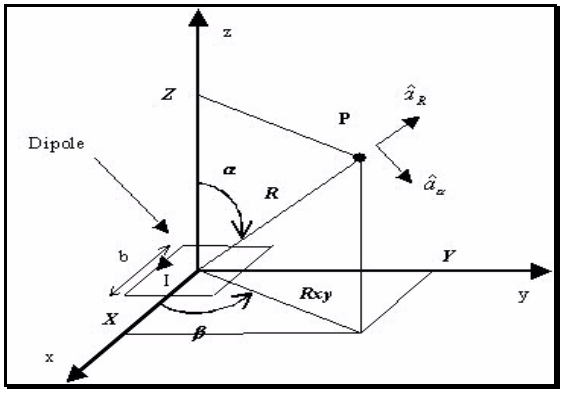

Fig. 2. Diagram for the dipole field equation

The magnetic field at a point P, produced by a square dipole at the origin (ref. Figure 2), is given by:

$$B = \frac{k_G}{R^3}[2\,\hat{a}_R \cos\alpha + \hat{a}_\alpha \sin\alpha]$$

where: B is the magnetic flux density (Tesla), R is the distance from the dipole to the point P (Metres), α is the angle from the coil axis to the point P (Radians), k_G is a constant equal to

$$\frac{\mu_0 NIb^2}{4\pi}$$

with $\mu_0 = 4\pi 10^{-7}$, N is the number of turns, I is the current inside the coil (Amps), b is the side of the coil (Metres), $\hat{a}_R$ is the unit vector in direction of R, $\hat{a}_\alpha$ is the unit vector in direction of α . Deriving the Cartesian form we obtain:

$$R = \sqrt{x^2 + y^2 + z^2}$$
$$R_{xy} = \sqrt{x^2 + y^2}$$
$$B_R = \frac{k_G}{R^3}(2\cos\alpha)$$
$$B_\alpha = \frac{k_G}{R^3}(\sin\alpha)$$

$$\cos\alpha = \frac{z}{R}$$
$$\sin\alpha = \frac{R_{xy}}{R}$$
$$\cos\beta = \frac{x}{R_{xy}}$$
$$\sin\beta = \frac{y}{R_{xy}}$$

Resolving the fields B_R and B_α:

$$B_{xy} = B_R \sin\alpha + B_\alpha \cos\alpha$$
$$= \frac{k_G}{R^3}[2\cos\alpha\sin\alpha + \sin\alpha\cos\alpha]$$
$$B_{xy} = \frac{k_G}{R^3}[3\cos\alpha\sin\alpha] = \frac{k_G}{R^3}\left[3\frac{zR_{xy}}{R^2}\right]$$
$$B_x = B_{xy}\cos\beta = \frac{k_G}{R^5}(3xz)$$
$$B_y = B_{xy}\sin\beta = \frac{k_G}{R^5}(3yz)$$
$$B_z = B_R\cos\alpha - B_\alpha\sin\alpha = \frac{k_G}{R^3}[2\cos^2\alpha - \sin^2\alpha]$$
$$= \frac{k_G}{R^5}[2z^2 - y^2 - x^2]$$

Combining the field components gives:

$$B = \frac{k_G}{R^5}[3z(\hat{a}_x x + \hat{a}_y y) + \hat{a}_z(2z^2 - y^2 - x^2)]$$

So for each generator coil, if the co-ordinates are (X_{Gi}, Y_{Gi}, $Z_{Gi}=0$), the magnetic field produced is:

$$B_{Gi} = \frac{k_G}{R^5}\begin{bmatrix} 3z(\hat{a}_x(x - X_{Gi}) + \hat{a}_y(y - Y_{Gi})) \\ + \hat{a}_z(2z^2 - (y - Y_{Gi})^2 - (x - X_{Gi})^2) \end{bmatrix}$$

where i is the index reference number for the generator coil. The e.m.f induced in the sensor coil when placed in a magnetic field is proportional to the resolved component of the field along its axis: $V_s = k_s(B.\hat{a}_s)$

where: V_S is the e.m.f induced in the sensor (Volts), k_S is a coefficient defining the sensitivity of the sensor (Volts per Tesla), $\hat{a}_S$ is the unit vector in direction of the sensor, which can be defined by the two angles θ and ϕ. Expressing the e.m.f induced in the sensor coil related to each generator coil (and their magnetic field), the following equation can be obtained:

$$V_{Si} = \frac{k_G k_S}{R^5}\begin{bmatrix} 3z\sin\theta((x - X_{Gi})\cos\phi + (y - Y_{Gi})\sin\phi) \\ + \cos\theta(2z^2 - (y - Y_{Gi})^2 - (x - X_{Gi})^2) \end{bmatrix}$$

From the nine different expressions of the above voltage equation (nine generator coils), x, y, z, θ, and ϕ, may be determined which are the only unknown variables in the equation.

III THE MATHEMATICAL MODEL

In order to measure the position and orientation of the hand in 3D space it is necessary to attach a set of sensors at strategic positions on a glove. Figure 3 shows the location of eleven miniature inductive sensors sown into a glove. These sensors are mounted on each finger-tip and the phalange above the base joint. One further sensor is put on the palm.

For further operation, we need to pre-define the fingers. Thumbs and Fingers are generically referred to as fingers. Fingers are numbered 0 to 4, where 0 is the thumb, and 4 is the little finger. Finger joints are numbered 0 to 3, where 0 is the base, and 3 is the finger tip.

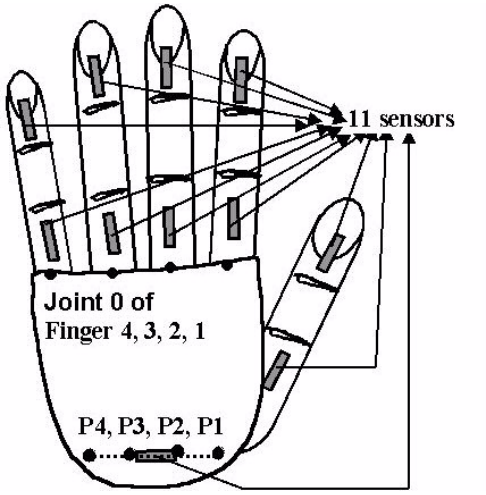

Fig. 3. Sensors Layout

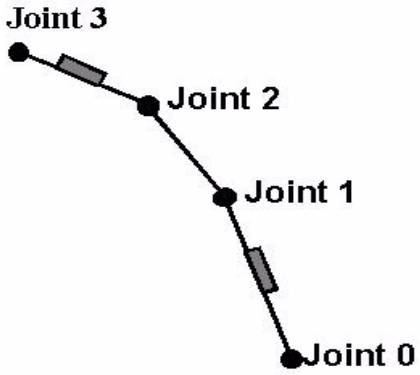

Fig. 4. Joint Positioning

3.1 Joint Positioning

First, the direction unit vector, converted from the orientation of S11 (ref. Figure 3), needs to be scaled by different factors, which is determined by the width of the wrist. Adding or subtracting the position vectors to S11, the position of P1, P2, P3, P4 could be worked out. The sensors, described above 'on each finger tip' and 'on the phalange above the finger base', are put along and in the middle of that phalange. Then positions of Joint 0, 1, 2, 3 of all finger 0, 1, 2, 3, 4 are determined by scaling the direction unit vector of the relevant sensor with the factor determined by the length of the phalange. The point 4, 3, 2, 1 and P4, P3, P2, P1 will be connected to form the basic quadrilateral prisms for drawing the palm.

3.2 Calculation of the Vertices for Each Face (8)

The shape of a human finger is cylindrical. To render a realistic image, the cylindrical shape is approximated as a series of octagonal prisms following the bending of a human finger. It is very easy to determine a plane in which the joint1 and 2 should lay by knowing their up vectors, which could be actually calculated by adding the direction vectors of the two finger bones linked by the proportional joint. Figure 6 shows the octagons constructed around the finger joints. Each of the eight vertices of neighboring octagons may be joined to form a series of connected quadrilateral prisms around the finger bone.

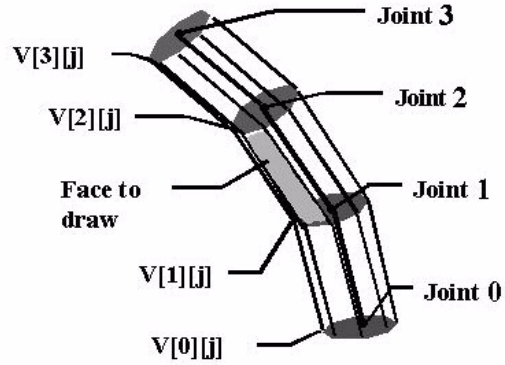

Fig. 5. The octagon shape used to represent the human finger phalanges.

3.3 Calculation of Facet and Surface Normals

After creating all the vertices, a series of four-side faces (ref. Figure 6) are available to define the finger surface. The series of faces are defined in counterclockwise in Open GL (the computer graphic library used in the program). For drawing the object in OpenGL the up-vector to each of these faces need to be calculated. And in order to make the image appears smooth surface normals should be calculated for each of the prism vertices by adding the facet normals of the four faces by which the vertex is share and then re-normalise.

3.4 Drawing the Object

Object Pascal-based graphics user interface Delphi-4 and Open-GL(for Open Graphic Library)are being used for rendering the image. Object Pascal is used as Object Oriented Programming Language in Delphi, which is based on three fundamental concepts: classes, inheritance and polymorphism (or later binding), event driving is the basic concept for programming. Open GL is a software interface designed for use with the C and C++ programming languages but there are also bindings for a number of other programming languages such as Pascal, Java, Tcl, Ada, FORTRAN. The interface consists of a set of several hundreds of procedures and functions allow a programmer to

specify the objects and operations involved in producing light-quality graphical images, specially the colour images of three-dimensional objects and render them into frame buffer. OpenGL is operating system and windowing system independent. It relies on the windowing system for window management, event handling, color map operations, etc. (8)

Figure 6 is the images captured from instances of a series real-time hand movement

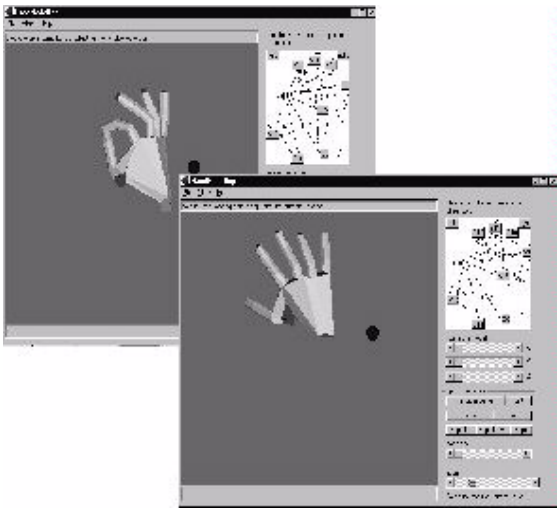

Fig. 6. 3D model

IV RESULTS AND THE ACCURACY OBTAINED

Each of the three sets of three generator coils generates a different time varying magnetic field (9). In total, 9 measurements of the induced voltage of a single sensor are available, therefore, the position parameter, x, y, z and orientation parameter θ and ϕ could be obtained. An algorithm has been developed to update the real time position and orientation parameters. There are multiple stages, stated as follows, in the internal process of getting from the electrical measurements (in volts and amps) to the final positions in metres. Each stage uses a calibration file to help convert from arbitrary units to SI units.

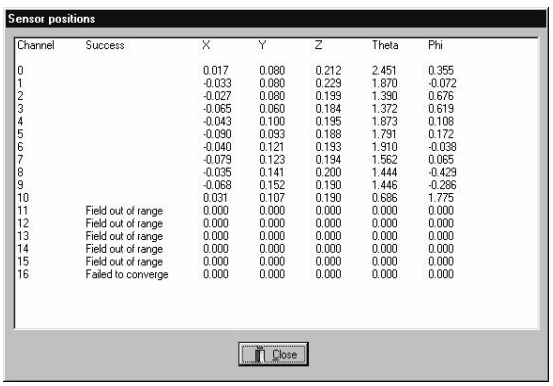

Sensor positions

Channel	Success	X	Y	Z	Theta	Phi
0		0.017	0.080	0.212	2.451	0.355
1		-0.033	0.080	0.229	1.870	-0.072
2		-0.027	0.080	0.199	1.390	0.676
3		-0.065	0.060	0.184	1.372	0.619
4		-0.043	0.100	0.195	1.873	0.108
5		-0.090	0.093	0.188	1.791	0.172
6		-0.040	0.121	0.193	1.910	-0.038
7		-0.079	0.123	0.194	1.562	0.065
8		-0.035	0.141	0.200	1.444	-0.429
9		-0.068	0.152	0.190	1.446	-0.286
10		0.031	0.107	0.190	0.686	1.775
11	Field out of range	0.000	0.000	0.000	0.000	0.000
12	Field out of range	0.000	0.000	0.000	0.000	0.000
13	Field out of range	0.000	0.000	0.000	0.000	0.000
14	Field out of range	0.000	0.000	0.000	0.000	0.000
15	Field out of range	0.000	0.000	0.000	0.000	0.000
16	Failed to converge	0.000	0.000	0.000	0.000	0.000

Close

Fig. 7. Sensor measurements in tabular form:
X,Y,Z are measured in metres; θ,φ in radians

Stage 1: Convert raw ADC data to volts

Stage2: Convert volts to "sensor volts per amp of drive current"

Stage 3: Apply calibration for the generator coils

Stage4: Apply calibration for sensor

Stage5: Convert result to signed magnitude

The algorithm provides the system fairly high accuracy

and reliability, this could be observed by putting the data-glove at a static position in the magnetic field and analyzing the vibration of position parameter, X, Y, Z and orientation parameter, θ and ϕ, of a randomly chosen sensor.

For example, when the data-glove is put statically at the position, which is indicated in Figure 7 above, the absolute vibration of X is 0.001 m, the same for Y and Z, and the absolute vibration value of θ is 0.001 ^{rads}, the same for ϕ.

Repeat this experiment and choose different sensors, the same results are obtained. By calculating the relative vibration percentage, the conclusion could be made that the accuracy of the system is higher than 99.5%.

V DATA RATE REQUIRED TO SUSTAIN A RELA-TIME MOVING AT THE REMOTE SITE

The image produced has to be redrawn regularly to give the impression of animation. This rate is called the refresh rate that is required to be 50 frames per second. It is governed by the capability of the system being used.

VI Strong ARM™ APPLICATION

ARM stands for Advanced RISC Machine, a name of company dedicated for RISC processor developing. ARM usually refers to a serial of 32-bit RISC cores designed by this company. The company of Advanced RISC Machine does not manufacture the ARM processors, but grants licenses to other semiconductor manufacturers. These manufactures either embed the ARM core into their own product, such as mobile phone, or integrated it with other modules to produce system-on-chip processor of ARM.

StrongARM is a kind of ARM processor from Intel[10]. It has powerful processor core running at up to 206MHz as well as rich set of on-chip resource, including MMU, LCD controller, UART, USB and etc. All these features lead to a compact and high performance solution. A prototype is developed as shown in Fig 8.

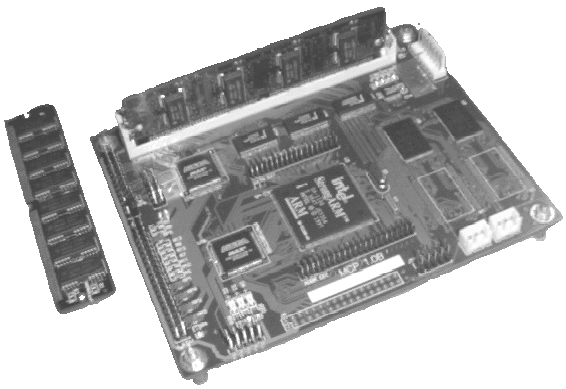

Fig. 8. StrongARM Prototype Board

A performance test for the 133 MHz StrongARM compared with a 266 MHz AMD K6-II processor is shown in Fig 9. It is conducted on eCos[11], an embedded operating system, using a 128 sample fixed-point FFT algorithm. When test program is full optimized with '-O3' option of compiler, the StrongARM is slightly faster than the 6x86 processor. The result relays heavily on the multiply-accumulate instruction of ARM processor[15]. Such kind of instructions can work efficiently in most digital processing applications. However, since StrongARM lacks on-chip float point hardware, its float point performance is very slow, only about 10% compared to the 6x86 processor.

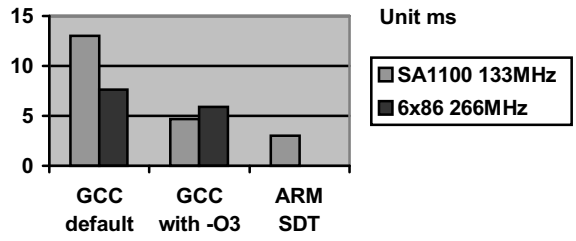

Fig. 9 Fix Point Performance

A new front-end signal processing algorithm will be implemented. In JSB system, nine coils are switched on sequentially and a matched filter used to measure the magnetic field component in the inductive coil sensor. In the new system, the nine generators are driven concurrently but with different frequencies. The sensor then detects all magnetic components simultaneously and this signal is frequency synthesized using a discrete Fourier transform.

A networked device can provide much more powerful functions, just imaging a computer with network and one without network. An Ethernet network interface[12] has been implemented on that StrongARM prototype board. In addition, an embedded web server [13] can work on this board providing web-based management and control. As a result, it would be possible for a doctor to make a diagnosis via the internet as easily as surfing the net with a web browser. Furthermore, wireless communication interface such as Bluetooth[14] is also considered.

Portable system can often bring additional convenience to the user. To make a portable system, following techniques are adopted or developed.

- Low power ICs, operating at 3.3V;
- Generator works at fine tuned frequency. A power PLL is designed to provide both efficiency and high accuracy in measurement.
- Power management software to monitor and control the power of whole system.
- Standard components, such as SODIMM DRAM, Smart Media Flash, are used to provide upgrade ability.
- Standard communication interface, such as Ethernet, USB, IrDA, UART and etc, are available to provide easy connection with remote or desktop system.

VII CONCLUSIONS

Sufficient visual reality has been obtained for capturing the hand motion from the above-described system. We introduced dynamics to a hand model by using the position and orientation parameter obtained from the sensors.

The application to Parkinson's Disease and Essential tremor will utilise the technology discribed above. By improving the current imaging system, hand motions of patients with the two most common movement disorders, essential tremor and Parkinson's disease could be realistically recorded and simulated for both clinical practice and research purpose.

REFERENCES

[1] Bain P, *Clinical measurement of tremor* Mov Disord , 13: 77-80, 1998.

[2] Bladen JS, Anderson AP, Bell GD, Rameh B, Evans B, Heatley DJT. *Non-radiological imaging of endoscopes.* Lancet 1993;341:719-722.

[3] Gibb WRG, Lees AJ. The relevance of the Lewy body to the pathogenesis of idiopathic Parkinson's disease. Journal of Neurology, Neurosurgery and Psychiatry 1988; 51: 745-752.

[4] Deuschl G, Zimmerman R, Genger H, Lucking CH. Physiologic classification of essential tremor. In: Findley LJ and Koller WC , editors. Handbook of tremor disorders. New York, NY: Marcel Dekker, 1995: 195-208.

[5] Pimental K, Teixeira K *Virtual Reality Through the new looking glass* Windcrest McGraw Hill 1992.

[6] Zubillaga-Elorza F, Allen CR, *Virtual Instrument Toolkit - Rapid prototyping on the Web*, IEEE Internet Computing, 4: 41-48, 1999.

[7] Bladen J.S: *Electromagnetic Imaging system for colonoscopy* PhD thesis, Sheffield University 1995.

[8] Ammeraal L: *Programming Principles in Computer Graphics, 2nd edition* Wiley Professional Computing 1992.

[9] Dogramadzi S, Allen CR, Bell GD, Rowland RS: *An Electromagnetic Imaging System For Remote Sign Language Communication* Proc. IEEE IMTC'99 Conference, Venice Italy 1443-1446 1999.

[10] Intel Corporation, *SA-1100 Microprocessor Technical Reference Manual*, September 1998.

[11] Red Hat, Inc., *eCos Reference Manual*, March 2000.

[12] Cirrus Logic, Inc., *CS8900A Product Data Sheet*, March 1999.

[13] GoAhead Software, *GoAhead WebServer Data Sheet*, April 1999.

[14] Ericsson Microelectronics AB, *PBA 313 01/2 Bluetooth Radio*, April 2000.

[15] ARM Limited, *ARM Architecture Reference Manual*, February 2000.